The dependence of the hole spectrum on spin frustration and direct hopping in the two-band Hubbard model

1991 J. Phys.: Condens. Matter 3 9129

(http://iopscience.iop.org/0953-8984/3/46/014)

J. Phys.: Condens. Matter 3 (1991) 9129–9139. Printed in the UK

The dependence of the hole spectrum on spin frustration and direct hopping in the two-band Hubbard model

A F Barabanov†, R O Kuzian† and L A Maksimov‡

† Institute for High Pressure Physics, 142092 Troitsk, Moscow Region, USSR

‡ Institute for Atomic Energy, 123182 Moscow, USSR

Received 13 March 1991, in final form 17 June 1991

Abstract. The one-hole spectrum $\varepsilon(k)$ in the CuO_2 plane is studied in the framework of the two-band Hubbard model with direct O–O hopping h. The finite O-hole concentration n is taken into account via the frustration α in the Cu spin subsystem. The $\varepsilon(k)$ minimum position and Fermi surface topology strongly depend on the α- and h-values. The density of states has a sharp peak near the bottom of the band. The model demonstrates the non-rigid-band behaviour of $\varepsilon(k)$ and Fermi level pinning observed in recent photoemission experiments on high-T_c superconductors.

1. Introduction

The angle-resolved photoemission and inverse photoemission experiments indicate the importance of electronic correlation effects in high-T_c superconductors (HTSCs) [1–4]. It is well known that many features of HTSCs are determined by doped CuO_2 planes. The experimental bands of these planes exhibit considerably less dispersion (about 500 meV) than one-electron band-structure calculations do [2, 5]. Spectroscopy studies demonstrate that the states at the Fermi level from CuO_2 doped planes are mainly O $2p_{x,y}$ states [6]. The empty Cu 3d states have predominantly $3d_{x^2-y^2}$ symmetry [7]. A realistic model for hole motion in the CuO_2 planes is the extended two-band Hubbard model proposed in [8–10]. It accounts for both Cu and O degrees of freedom. In the strong-coupling limit it is possible to project onto basis states in which each Cu site has a spin $\frac{1}{2}$ and the holes are restricted to O sites. Then the effective Hamiltonian describes the O-hole hoppings over the Cu sites and the hole motion strongly depends on the Cu spin subsystem state $|G\rangle$. The analogous reduction of the single-band large-U Hubbard model leads to the so-called t–J (or t–t'–J) model. In either case, first of all one is interested in describing the low-energy band which is responsible for conductivity and superconductivity in hole-doped HTSCs.

Because of strong coupling between the hole and the surrounding Cu spins the hole must be treated as a magnetic polaron and the problem is extremely difficult. Usually one solves the case of one hole without explicit consideration of hole–hole interaction.

In the present work we restrict our attention to the one-hole spectrum $\varepsilon(k)$ in the framework of the two-band Hubbard model in the case of a small magnetic polaron radius. The most interesting previous result is that approximately

$$\varepsilon(k) \propto \gamma_k^2 \qquad \gamma_k \equiv \tfrac{1}{2}[\cos(k_x g) + \cos(k_y g)] \tag{1}$$

where g is the Cu sublattice constant. The spectrum (1) was obtained in both analytical

0953-8984/91/469129 + 11 $03.50

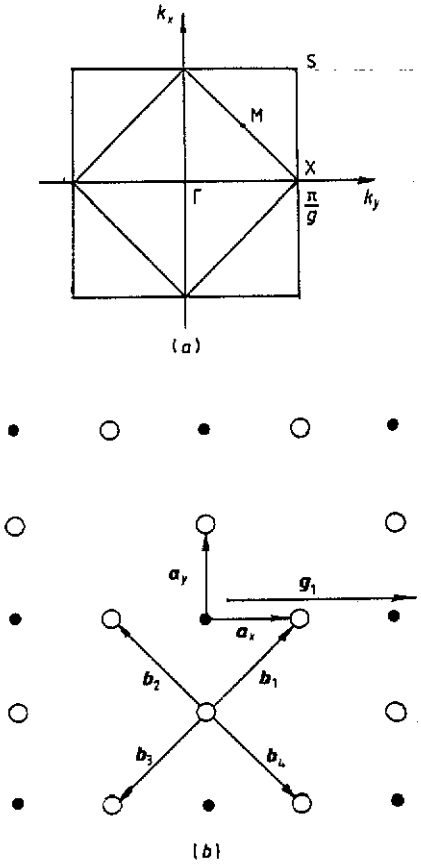

Figure 1. (*a*) The full and the magnetic (reduced) Brillouin zone for CuO_2. (*b*) The CuO_2 plane structure: ●, Cu sites; ○, O denotes sites. a_x and a_y are the O-site vectors in the unit cell; b_{1-4} are the NN vectors on the O sublattice.

[11–16] and numerical [13, 14] approaches. To get (1), one needs to assume not too small Cu–Cu exchange J compared with effective O hopping τ. This assumption restricts the size of the polaron. It is interesting that spectrum (1) is true for two different types of states $|G\rangle$: for the Néel-type state with two magnetic sublattices and with $\langle \hat{S}_R^z \rangle \neq 0$ ($\hat{S}_R^z$ is the Cu spin projection operator on site R) [11–16] and for the RVB-type singlet Cu spin state with $\langle \hat{S}_R^z \rangle = 0$ [14, 15]. Let us remember that a common feature of these states is the short-range antiferromagnetic (AFM) order.

The bottom of the hole band (1) lies at the magnetic zone boundary (figure 1(*a*)) where $\gamma_k = 0$, and the density $\rho(\varepsilon)$ of states has a quasi-one-dimensional singularity near the bottom of the band. Accurate calculations which take into account the detailed structure of the state $|G\rangle$ and direct O–O hopping modulate $\varepsilon(k)$ (1) [13, 15]. The local minima appear near the magnetic zone boundary and equienergetic lines can have a non-trivial shape. On the other hand, if the simplest possible assumption is made that the quasi-particles fill the rigid band described by the single hole $\varepsilon(k)$, forming a weakly interacting Fermi gas, then the above-mentioned details of spectrum are important. For example, these details can qualitatively determine the sign of the Hall resistivity [17, 18].

The motivation for the present study is to obtain more conclusive results for the O-hole band structure, when we take into account both the direct O–O hopping h and the finite doping. We assume the Cu subsystem state $|G\rangle$ to be the singlet. We believe that the main influence of finite but small doping consists in the modification of the spin

correlation functions in the state $|G\rangle$. The latter modifies the $\varepsilon(k)$ spectrum. As has been shown for the one-band Hubbard model [19], the doping is equivalent to frustration in the Cu–Cu interaction, i.e. the AFM interaction between next-nearest neighbours (NNN) in the Cu sublattice. So we allow for doping by including the frustration.

The paper is organized as follows. In section 2 we introduce the effective Hamiltonian, formulate our main assumptions and the method of $\varepsilon(k)$ calculation. In section 3 we give the lowest-band $\varepsilon(k)$ results for different values of frustration parameter α and direct O–O hopping h. The matrix elements of the effective Hamiltonian are presented in the appendix. The conclusion contains a brief discussion of the results.

2. The method of spectrum calculation

The Hamiltonian of an extra hole in the extended Hubbard model for the CuO_2 lattice is [11, 20]

$$\hat{H} = \hat{T} + \hat{H}_J + \hat{h} \tag{2}$$

$$\hat{T} = \sum_{R,a_1,a_2,\sigma} \{[\tau + \delta_{a_1,a_2}(\tau_1 - \tau)]\, Z_R^{\sigma_1\sigma_2}\} c^+_{R+a_2,\sigma_2} c_{R+a_1,\sigma_1}$$

$$a_1, a_2 = \pm a_x, \pm a_y$$

$$\hat{H}_J = \hat{J}_1 + \hat{J}_2 \qquad \hat{J}_1 = J \sum_{R,g} \hat{S}_R \cdot \hat{S}_{R+g} \qquad \hat{J}_2 = \alpha J \sum_{R,d} \hat{S}_R \cdot \hat{S}_{R+d}$$

$$\hat{h} = -h \sum_{R,a=a_x,a_y,b} c^+_{R+a} c_{R+a+b}$$

$$\tau = t^2/\varepsilon \qquad \tau_1 = t^2/(\varepsilon + U_p).$$

Here and below $\boldsymbol{R} + \boldsymbol{a}$ are four vectors of O sites nearest to the Cu site $\boldsymbol{R}$; $\boldsymbol{b}$ are nearest-neighbour (NN) vectors for the oxygen sublattice; $\boldsymbol{g} = 2\boldsymbol{a}$ and $\boldsymbol{d} = 2\boldsymbol{b}$ are the first- and second-NNs for the Cu sublattice (see figure 1(*b*)); the operators c^+_σ and $Z^{\sigma 0}$ create a hole with spin index $\sigma = \pm 1$ at the O and Cu sites, respectively, and $Z_R^{\sigma_1\sigma_2}$ are the Hubbard projection operators which are convenient for excluding doubly occupied Cu sites.

The first term $\hat{T}$ in (2) describes the effective hole hoppings from O to O sites through the intervening Cu sites. The distinctive feature of the $\sigma_1 \neq \sigma_2$ hopping terms in $\hat{T}$ consists of a simultaneous spin flip of O and Cu holes. The term $\hat{J}_1$ represents the NN AFM Cu–Cu interaction.

The $\hat{T}$- and $\hat{J}_1$-terms can be obtained in the framework of perturbation theory in $t/\varepsilon \ll 1$ from the site Hamiltonian which is characterized by the Cu and O hole levels ε_d and ε_p ($\varepsilon = \varepsilon_p - \varepsilon_d > 0$), by the NN Cu–O hopping t and by the intrasite Hubbard repulsion energies U_d and U_p for Cu and O respectively. We put $U_d = \infty$ as a largest energy parameter.

The term $\hat{J}_2$ describes the AFM interaction between second-NN Cu spins, i.e. the frustration with an effective parameter α. As we mentioned above, the increase in α we connect with the increase in hole doping concentration n in the CuO_2 plane.

The last summation $\hat{h}$ allows for the direct O–O NN hopping.

From estimates of typical Hubbard model parameters [21, 22] one can find that $h < \tau \propto 0.5$ eV, $U_p \ll U_d$, and below we take $U_p = 0$, $J \simeq 0.25\tau$; we took the frustration parameter α to be 0.35 or less.

The hole excitation in the two-band Hubbard model is known to be a magnetic polaron [11–16]. Its wavefunction ψ explicitly contains the Cu spin subsystem wavefunction $|G\rangle$. For an excitation with $\sigma = +1$, ψ can be written in the most general form as

$$\psi = \sum_{\boldsymbol{R},\boldsymbol{a}=\boldsymbol{a}_x,\boldsymbol{a}_y} \beta(\boldsymbol{R},\boldsymbol{a})\varphi^+(\boldsymbol{R},\boldsymbol{a})|G\rangle \tag{3}$$

$$\begin{aligned}\varphi^+(\boldsymbol{R},\boldsymbol{a}) = c^+_{\boldsymbol{R}+\boldsymbol{a},+1}\Big(&f_0(\boldsymbol{R},\boldsymbol{a}) + \sum_{\boldsymbol{R}_1,\sigma} f_1(\boldsymbol{R},\boldsymbol{a},\boldsymbol{R}_1,\sigma)Z^{\sigma\sigma}_{\boldsymbol{R}_1} \\ &+ \sum_{\boldsymbol{R}_1,\boldsymbol{R}_2\sigma_1-\sigma_2+\sigma_3-\sigma_4=0} f_2(\boldsymbol{R},\boldsymbol{a},\boldsymbol{R}_1,\boldsymbol{R}_2,\sigma_1,\sigma_2,\sigma_3,\sigma_4)Z^{\sigma_1\sigma_2}_{\boldsymbol{R}_1}Z^{\sigma_3\sigma_4}_{\boldsymbol{R}_2} + \ldots\Big) \\ + c^+_{\boldsymbol{R}+\boldsymbol{a},-1}\Big(&g_0(\boldsymbol{R},\boldsymbol{a}) + \sum_{\boldsymbol{R}_1} g_1(\boldsymbol{R},\boldsymbol{a},\boldsymbol{R}_1)Z^{+-}_{\boldsymbol{R}_1} \\ &+ \sum_{\boldsymbol{R}_1,\boldsymbol{R}_2,\sigma_1-\sigma_2+\sigma_3-\sigma_4=2} g_2(\boldsymbol{R},\boldsymbol{a},\boldsymbol{R}_1,\boldsymbol{R}_2,\sigma_1,\sigma_2,\sigma_3,\sigma_4)Z^{\sigma_1\sigma_2}_{\boldsymbol{R}_1}Z^{\sigma_3\sigma_4}_{\boldsymbol{R}_2} + \ldots\Big).\end{aligned}$$

The wavefunction (3) explicitly takes into account the fact that during the motion an oxygen hole may change its spin projection (terms with coefficients g_i) and create an irregular copper spin order with respect to $|G\rangle$ (terms with $Z^{+-}_{\boldsymbol{R}}$ and $Z^{-+}_{\boldsymbol{R}}$ operators).

As has been shown in [15] for the case of the Néel Cu subsystem spin state and for realistic values of $J \propto 0.25\tau$, the carrier spectrum is correctly described in the framework of the magnetic polaron of small radius. We use this small-radius approximation which means that one can retain in (3) the terms of zero and first order in $Z_{\boldsymbol{R}_1}$ operators only and can keep the sites $\boldsymbol{R}_1$ nearest to the O-hole site $\boldsymbol{R}+\boldsymbol{a}$, i.e. $\boldsymbol{R}_1 = \boldsymbol{R}$, $\boldsymbol{R}+2\boldsymbol{a}$. It is convenient to use the trial functions φ which are the eigenfunctions of total spin square $\hat{S}^2$ of the system (O hole and Cu spins) and its projection $\hat{S}^z$. Detailed investigation of small clusters shows that the lowest hole band for the model under consideration is determined by the $S = \frac{1}{2}$ polaron state. Then a complete basis set for the $S = \frac{1}{2}$ localized polaron of small radius is

$$\begin{aligned}\varphi_{i\boldsymbol{R}} &= \hat{\varphi}^+_{i\boldsymbol{R}}|G\rangle \qquad i = 1\text{–}6 \\ \hat{\varphi}^+_1 &= c^+_{\boldsymbol{R}+\boldsymbol{a}_x,+1}Z^{--}_{\boldsymbol{R}} - c^+_{\boldsymbol{R}+\boldsymbol{a}_x,-1}Z^{+-}_{\boldsymbol{R}} \\ \hat{\varphi}^+_2 &= c^+_{\boldsymbol{R}+\boldsymbol{a}_y,+1}Z^{--}_{\boldsymbol{R}} - c^+_{\boldsymbol{R}+\boldsymbol{a}_y,-1}Z^{+-}_{\boldsymbol{R}} \\ \hat{\varphi}^+_3 &= c^+_{\boldsymbol{R}+\boldsymbol{a}_x,+1}Z^{--}_{\boldsymbol{R}+2\boldsymbol{a}_x} - c^+_{\boldsymbol{R}+\boldsymbol{a}_x,-1}Z^{+-}_{\boldsymbol{R}+2\boldsymbol{a}_x} \\ \hat{\varphi}^+_4 &= c^+_{\boldsymbol{R}+\boldsymbol{a}_y,+1}Z^{--}_{\boldsymbol{R}+2\boldsymbol{a}_y} - c^+_{\boldsymbol{R}+\boldsymbol{a}_y,-1}Z^{+-}_{\boldsymbol{R}+2\boldsymbol{a}_y} \\ \hat{\varphi}^+_5 &= c^+_{\boldsymbol{R}+\boldsymbol{a}_x,+1} \\ \hat{\varphi}^+_6 &= c^+_{\boldsymbol{R}+\boldsymbol{a}_y,+1}.\end{aligned} \tag{4}$$

Here $\boldsymbol{R}$ denotes the unit cell where the O hole is localized, and $\boldsymbol{R}+\boldsymbol{a}_{x(y)}$ are two oxygen site locations in the unit cell $\boldsymbol{R}$ (see figure 1(*b*)).

The functions (4) are normalized if one takes into account that $\langle Z^{++}\rangle = \langle Z^{--}\rangle = \frac{1}{2}\langle\ldots\rangle \equiv \langle G|\ldots|G\rangle$. Using the singlet character of state $|G\rangle$ it is easy to verify that $\hat{S}^2\varphi_{i\boldsymbol{R}} = \varphi_{i\boldsymbol{R}}$; $\hat{S}^z\varphi_{i\boldsymbol{R}} = \frac{1}{2}\varphi_{i\boldsymbol{R}}$.

The basis set (4) is not orthogonal, e.g. $\langle\varphi_{1\boldsymbol{R}}|\varphi_{3\boldsymbol{R}}\rangle = \langle Z^{--}_{\boldsymbol{R}}Z^{--}_{\boldsymbol{R}+2\boldsymbol{a}}\rangle + \langle Z^{-+}_{\boldsymbol{R}}Z^{+-}_{\boldsymbol{R}+2\boldsymbol{a}}\rangle$.

We shall search for the polaron spectrum ε_k by means of the variational method:

$$\varepsilon_k = \frac{\langle\varphi_k\hat{H}\varphi^+_k\rangle}{\langle\varphi_k|\varphi_k\rangle} \qquad \hat{\varphi}^+_k = \sum_i f_{ik}\hat{\varphi}^+_{ik} \qquad \hat{\varphi}^+_{ik} = N^{-1}\sum_{\boldsymbol{R}}\exp(i\boldsymbol{k}\cdot\boldsymbol{R})\,\hat{\varphi}^+_{i\boldsymbol{R}} \tag{5}$$

where N is the number of Cu sites and f_{ik} are variational coefficients. The secular equation

matrix elements contain two-site and three-site Z-operator correlation functions which are determined by the $|G\rangle$ state structure. Owing to the singlet nature of $|G\rangle$ these correlations can be expressed through the pair spin correlations between first, second and third Cu NNs. Let us give the expressions for some typical correlations which enter the secular equation:

$$\langle Z_1^{++} Z_2^{--} \rangle = \langle (\tfrac{1}{2} + S_1^z)(\tfrac{1}{2} - S_2^z) \rangle = \tfrac{1}{4} - \tfrac{1}{2}\langle S_1^z \rangle + \langle S_2^z \rangle \tfrac{1}{2} - \langle S_1^z S_2^z \rangle = \tfrac{1}{4} - \tfrac{1}{3}\langle S_1 \cdot S_2 \rangle$$

$$\langle Z_1^{+-} Z_2^{++} Z_3^{-+} \rangle = \langle Z_1^{+-} Z_3^{-+} \rangle - \langle Z_1^{+-} Z_2^{--} Z_3^{-+} \rangle = \langle Z_1^{+-} Z_3^{-+} \rangle - \langle Z_1^{-+} Z_2^{++} Z_3^{+-} \rangle$$

$$= \langle Z_1^{+-} Z_3^{-+} \rangle - \langle Z_1^{+-} Z_2^{++} Z_3^{-+} \rangle = \tfrac{1}{2}\langle Z_1^{+-} Z_3^{-+} \rangle$$

$$\langle Z_1^{+-} Z_3^{-+} \rangle = \tfrac{1}{2}\langle Z_1^{+-} Z_3^{-+} + Z_1^{-+} Z_3^{+-} \rangle = \langle S_1^x S_3^x + S_1^y S_3^y \rangle = \tfrac{2}{3}\langle S_1 \cdot S_3 \rangle.$$

The explicit form of Hamiltonian and overlap matrix elements is given in the appendix.

To find the spin correlations, one has to consider the ground state and spin excitation problem for the Hamiltonian $\hat{H}_J$ (2), which corresponds to the two-dimensional $S = \frac{1}{2}$ AFM Heisenberg model with frustration on the square lattice. To describe the singlet state $|G\rangle$, one needs to use a spherically symmetric theory which gives $\langle S_0^\alpha S_R^\beta \rangle = \delta_{\alpha\beta} K(R)/3$. Such a theory based on site spin operator replacement by Schwinger bosons is developed in [23]. However, this theory uses the one-site 'constraint in average' and that is why the spin correlations happen to be overestimated by $\frac{3}{2}$ times.

We shall use the results of another method [24] which is devoid of the above-mentioned shortcomings. The method treats the spin excitations in terms of four spin block eigenstates which take into account short-range spin correlation in the zero approximation. The spin correlation dependence on the frustration parameter α can be expressed over the spin excitation Green functions given in [24]. For simplicity we assume that the pair site correlations between the second- and the third-NN Cu spins coincide, i.e. $K(2a_x + 2a_y) = K(4a_x) = K_2$. This approximation is known to be good at least for $\alpha = 0$ [25]. Let us represent the calculated values of spin correlations for several frustration parameter values $\alpha = 0$, 0.2 and 0.35, $K_1 = -0.324$, -0.297 and -0.268, and $K_2 = 0.221$, 0.169 and 0.102. The properties of the state $|G\rangle$ are discussed in [24] in detail and here we shall only mention that at $\alpha = 0.25$ there is a transition from a long-range order state to the spin liquid state at zero temperature.

3. Hole excitation spectrum

We represent $\varepsilon(k)$ only for the most interesting lowest band. To clarify the genesis of subsequent different types of $\varepsilon(k)$ spectrum, firstly we consider the case which can be treated analytically. Let us put the direct hopping $h = 0$ and choose a particular symmetric combination of variational wavefunctions φ_i^+, $i = 1$–4, from (4):

$$\theta_R = \tfrac{1}{2} \sum_{a = \pm a_x, \pm a_y} (c_{R+a,+1}^+ Z_R^{--} \mp c_{R+a,-1}^+ Z_R^{+-})|G\rangle. \tag{6}$$

The θ_R-function is an analogue of one oxygen-hole singlet ground state for a cluster with one Cu and four O sites [11, 26]. With the θ_R-functions, one can obtain the analytic expression for the spectrum:

$$\varepsilon(k) = -3.5\tau - [4J(A_3 + \alpha A_4) + (4.5A_1\tau - A_3 J)\gamma_k + A_2\tau(1 - 4\gamma_k^2)](1 + A_1\gamma_k)^{-1} \tag{7}$$

$$A_1 = \tfrac{1}{4} + K_1 \qquad A_2 = \tfrac{1}{8} - K_1 + \tfrac{1}{2}K_2 \qquad A_3 = 2K_1 \qquad A_4 = 2K_2.$$

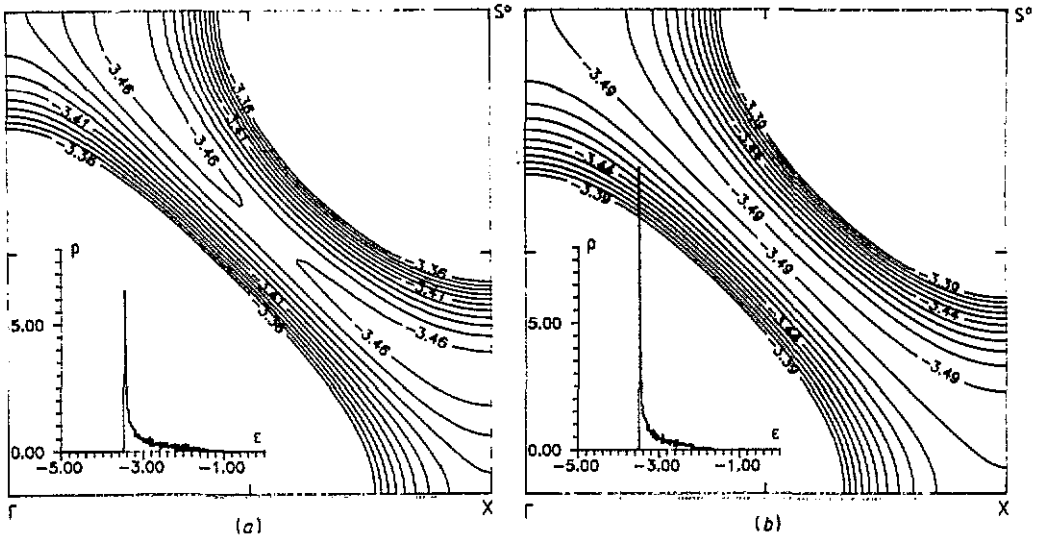

Figure 2. Equienergy lines $\varepsilon(k)$ = constant ($\tau = 1$) for zero O–O hopping $h = 0$: (*a*) without frustration, $\alpha = 0$; (*b*) frustration parameter $\alpha = 0.35$. The values of O-hole concentration n are given in parentheses. The density $\rho(\varepsilon)$ of states is plotted in the insets.

Here and below the polaron energy is counted off from the $|G\rangle$-state magnetic energy.

If one omits terms of the order of $J/\tau < 1$ in the spectrum (7), then the NN polaron hoppings would be determined by the coefficient A_1 which depends on the correlation K_1. On the other hand the important property of state $|G\rangle$ is that in a wide range of frustration parameters α the correlation K_1 is close to -0.25 and $|A_1| \ll 1$. Then, as a consequence, in the first approximation ($A_1 \simeq 0$) the spectrum (7) reduces to (1).

The spectrum $\varepsilon(k)$ (7) has no local minima. The minimum of $\varepsilon(k)$ is achieved along the equienergy line defined by the equation $\gamma_k \propto A_1/A_2$. For small doping and for $A_1 \ll A_2$ the spectrum is of electronic type.

Let us represent the results of $\varepsilon(k)$ calculations by the basis set (4). Firstly we consider the influence of frustration α on the spectrum in the case $h = 0$. The equienergy lines $\varepsilon(k)$ = constant and the corresponding band filling (n is the concentration of oxygen holes per two spin projections) for $\alpha = 0$ are shown in figure 2(*a*), and those for $\alpha = 0.35$ are given in figure 2(*b*). The densities $\rho(\varepsilon)$ of states are presented in the insets. It may be seen that in both cases the density $\rho(\varepsilon)$ of states has a sharp maximum near the bottom of the band; this is analogous to the quasi-one-dimensional singularity of the spectrum (1). To demonstrate $\varepsilon(k)$ peculiarities throughout the whole Brillouin zone we represent in figure 3 the spectrum along the principal axis.

In the absence of frustration the spectrum $\varepsilon(k)$ has local minima on the Brillouin zone boundary. In the rigid-band approximation and for small concentrations n the Fermi lines form four-hole closed pockets (OZ dispersion is absent and the Fermi surface is a cylinder defined by the Fermi lines in the k_x–k_y plane). When the concentration n increases, some parts of the Fermi lines change their signs of curvature from hole to electronic type; see, for example, the $\varepsilon = -3.46\tau$ ($n = 0.12$) line in figure 2(*a*). For large band fillings the Fermi lines change their topology and become purely electronic. If following [17, 18] we suppose that the magnetic polarons form a weakly interacting Fermi gas, then this topology transition must lead to a Hall resistivity sign change.

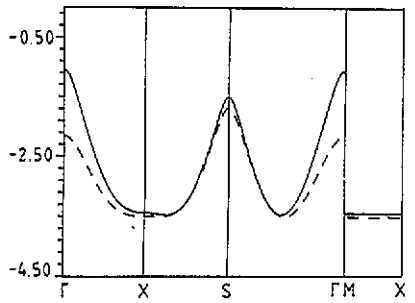

Figure 3. The spectrum $\varepsilon(k)$ along the principal axis in the Brillouin zone for $h = 0$: ——, $\alpha = 0$; – – –, $\alpha = 0.35$.

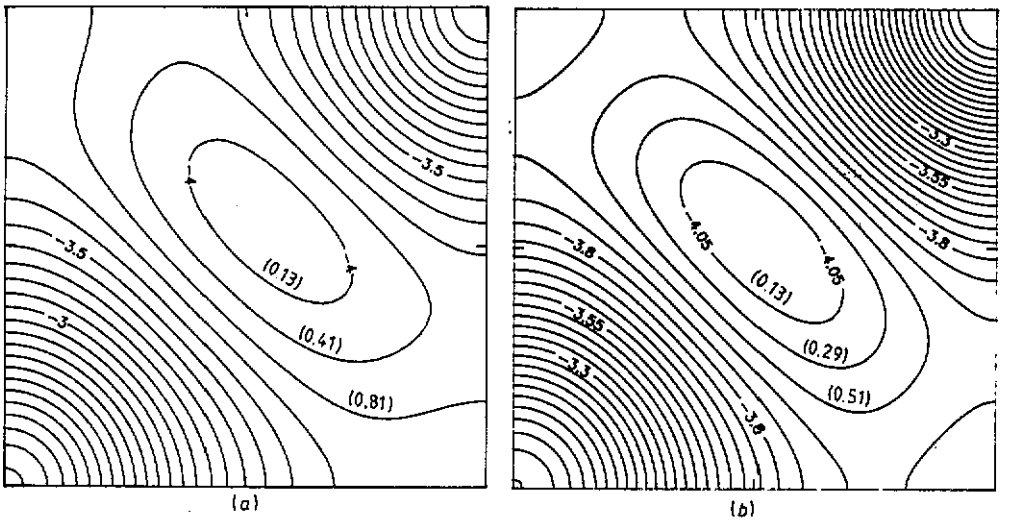

Figure 4. Equienergy lines $\varepsilon(k)$ = constant ($\tau = 1$) for O–O hopping $h = 0.3$: (*a*) without frustration, $\alpha = 0$; (*b*) frustration parameter $\alpha = 0.35$. The values of O-hole concentration n are given in parentheses.

The frustration changes the hole spectrum essentially, as is seen from figure 2(*b*). As α increases, the local minima move towards the points $gk = (\pm\pi, 0)$, $(0, \pm\pi)$ and become less pronounced and in figure 2(*b*) they are indistinguishable. The Fermi line transformation from hole to electronic type takes place at a concentration value n appreciably less than that for $\alpha = 0$. For example this change occurs at $n = 0.09$ for $\alpha = 0.35$. So we can conclude that at $h = 0$ the frustration drives $\varepsilon(k)$ close to the spectrum (1).

Let us discuss the influence of direct O–O hopping h. Figures 4(*a*) and 4(*b*) represent the equienergy lines and corresponding band fillings at $\alpha = 0$ and 0.35, respectively, for $h = 0.3$. The densities of states are given in figure 5 and the dispersions along the symmetry directions are shown in figure 6. It can be seen that the $\varepsilon(k)$ minimum is removed to the line ΓS and is placed near $gk = (\pi/2, \pi/2)$ relative to the case $h = 0$. The equienergy lines have a complex shape but as before the concentration increase drives the hole–electron transition of the Fermi line curvature. The frustration moves the minimum closer towards $gk = (\pi/2, \pi/2)$.

If we take into account that the increase in n leads to the increase in frustration, then we make sure of the following peculiarity of the magnetic polaron spectrum: the Fermi energy shift with doping is much less in magnitude than predicted by the rigid-band

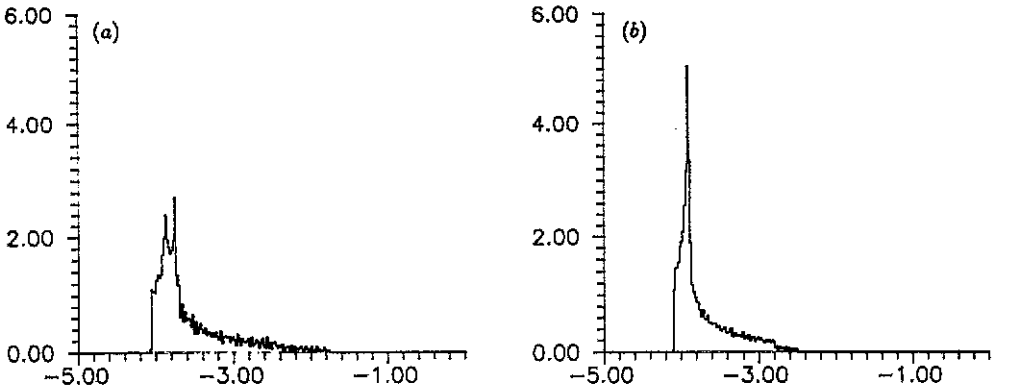

Figure 5. The density of states for the spectra shown in figure 4 ($h = 0.3$): (*a*) $\alpha = 0$; (*b*) $\alpha = 0.35$.

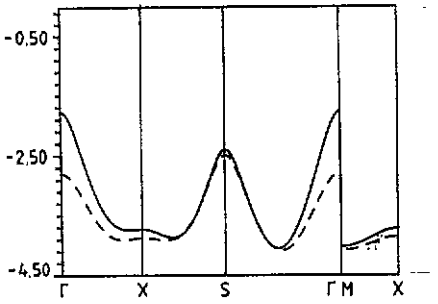

Figure 6. The spectrum $\varepsilon(k)$ along the principal axis in the Brillouin zone for $h = 0.3$: ——, $\alpha = 0$; – – –, $\alpha = 0.35$.

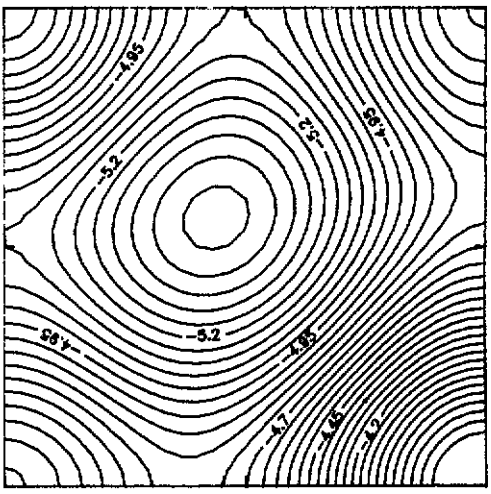

Figure 7. Equienergetic lines $\varepsilon(k)$ = constant for $h = \tau$ without frustration.

model; moreover the shift can have an opposite sign. Indeed, if we suppose that $\alpha = 0.35$ for $n = 0.1$ (this estimate is based on the one-band Hubbard model [19], $U/t \propto 5$) and $\alpha = 0$ for $n = 0$, then for the case $h = 0$ we have $\varepsilon_F(n = 0) = -3.48\tau \simeq \varepsilon_F(n = 0.1) = -3.49\tau$. For $h = 0.3$, $\varepsilon_F(n = 0) = -4.06\tau \simeq \varepsilon_F(n = 0.1) \simeq -4.06\tau$.

To clarify the tendency of the $\varepsilon(k)$ transformation with h increase we represent the spectrum for $h = \tau$ and $\alpha = 0$ in figure 7. The minimum $\varepsilon(k)$ is not shifted from the $gk = (\pi/2, \pi/2)$ region. However, there is a decrease in the $\varepsilon(k)$ anisotropy near the bottom of the band. Let us mention that, for $h \propto \tau$, one must take into account O p_π orbitals which are perpendicular to p_σ ($p_{x,y}$) orbitals.

4. Conclusion

We shall summarize the main results of our $\varepsilon(k)$ calculation for the small-radius magnetic polaron. For small direct hopping ($h \simeq 0$) and in a rather wide range of frustration

parameter values ($\alpha \leqslant 0.35$) the magnetic polaron moves predominantly on one Cu magnetic sublattice. This is the consequence of the spin correlations in the Cu subsystem singlet state $|G\rangle$. The correlations suppress the NN polaron hopping amplitude ($A_1 \ll 1$ in spectrum (6)). As a result, $\rho(\varepsilon)$ has a sharp peak near the bottom of the band. The $\varepsilon(\boldsymbol{k})$ minimum lies near the Brillouin zone boundary XS. The direct O–O hopping moves the bottom of the band to the vicinity of the point M $(\pi/2, \pi/2)$.

The inclusion of frustration enhances the spectrum anisotropy and $\rho(\varepsilon)$ peak intensity. We demonstrate the non-rigid-band behaviour concerning the shift of the Fermi level position on doping if we take into account the frustration parameter dependence on the hole concentration. This can explain the Fermi level pinning which was observed in HTSC photoemission experiments [3, 4].

In accordance with the experimental results on the Hall effect [27], the calculated Fermi lines change the topology and the sign of curvature with doping.

Let us mention the well known close correspondence between the spectra of magnetic polaron in the model under consideration and the t–J, t–t'–J models (see [28–30] and references therein).

Finally, we discuss the conjecture taken above about the equivalence of the doping to the frustration in the spin subsystem manifested in [19]. Recently this equivalence has been supported by the straightforward 4×4 cluster calculation of static spin–spin structure factor $S(\boldsymbol{q})$ for both doped t–J and J_1–J_2–J_3 frustrated spin-$\frac{1}{2}$ Heisenberg 2D models [31]. Our variational approximation for $\varepsilon(\boldsymbol{k})$ (5) contains only the static correlations; so the above conjecture seems to be legitimate. As to the dynamic magnetic behaviour of doped systems, recently it was shown that it cannot be accurately modelled by a purely spin Hamiltonian; the doped t–J and frustrated J–J' models give different results for the dynamic spin–spin structure factor $S(\boldsymbol{q}, \omega)$ and the Raman scattering spectrum $R(\omega)$ [32]. For the more realistic two-band Hubbard model we must mention the phenomenological frustration models [33, 34] where the spin–hole coupling creates a ferromagnetic exchange between neighbouring Cu spins. Among the microscopic investigations we must point out the result of [35] where the frustration in the spin subsystem is due to the direct O–O hopping. Nevertheless the question about the equivalence remains to be studied despite the above-mentioned achievements.

Appendix

Here we represent the Hamiltonian H_{ij} and overlap S_{ij} matrices in the basis φ_{ik} (5). If we take into account that $|G\rangle$ is an eigenfunction of the Hamiltonian $\hat{H}_J$ with the eigenvalue E_G, it is convenient to give the secular equation matrix elements in the following form:

$$H_{ij} - E_k\langle\varphi_{ik}\varphi_{jk}^{+}\rangle = \langle\varphi_{ik}[\hat{H}, \varphi_{ik}^{+}]\rangle - (E_k - E_G)\langle\varphi_{ik}\varphi_{ik}^{+}\rangle$$
$$\equiv B_{ij} - \varepsilon_k S_{ij}, \quad \varepsilon(\boldsymbol{k}) = E_k - E_G.$$

To simplify B_{ij}, S_{ij} we introduce the phase factor $\exp(\mathrm{i}\boldsymbol{k}\cdot\boldsymbol{a}_x)$ for φ_{jk} with odd j and $\exp(\mathrm{i}\boldsymbol{k}\cdot\boldsymbol{a}_y)$ for even j. After some algebra we obtain for B_{ij}, $(\tau = 1, g = 1)$

$$B_{11} = -\tfrac{1}{2} - 2A_1\cos(k_x) - 12J(A_3 + \alpha A_4)$$

$$B_{21} = -\{\exp[\mathrm{i}(k_x - k_y)/2] + 2A_1\cos[(k_x + k_y)/2] - A_2\exp[-\mathrm{i}(k_x - k_y)/2]\}$$
$$- h\{\exp[\mathrm{i}(k_x - k_y)/2] + 2A_1\cos[(k_x + k_y)/2]$$
$$+ A_5\exp[-\mathrm{i}(k_x - k_y)/2]\}$$

$$B_{31} = -2A_1 - [\exp(ik_x) - A_2 \exp(-ik_x)] + 3JA_3$$

$$B_{41} = -\{\exp[i(k_x + k_y)/2] + 2A_1 \cos[(k_x - k_y)/2] - A_2 \exp[-i(k_x + k_y)/2]\}$$
$$-h\{\exp[i(k_x + k_y)/2] + 2A_1 \cos[(k_x - k_y)/2]$$
$$- A_5 \exp[-i(k_x + k_y)/2]\}$$

$$B_{51} = -\exp(ik_x)/2 + A_6 \exp(-ik_x) - A_1$$

$$B_{61} = -\exp[i(k_x - k_y)/2] + 2A_6 \exp[-i(k_x + k_y)/2] + A_6 \exp[-i(k_x - k_y)/2]$$
$$- \exp[i(k_x + k_y)/2]/2 - h\{\cos[(k_x - k_y)/2] + \cos[(k_x + k_y)/2]\}$$

$$B_{55} = 1 + \cos(k_x)$$

$$B_{56} = \cos[(k_x + k_y)/2] + \cos[(k_x - k_y)/2]$$
$$- 2h\{\cos[(k_x + k_y)/2] + \cos[(k_x - k_y)/2]\}$$

$$A_1 = \tfrac{1}{4} + K_1 \qquad A_2 = \tfrac{1}{8} - K_1 + \tfrac{1}{2}K_2 \qquad A_3 = 2K_1 \qquad A_4 = 2K_2$$

$$A_5 = K_2 + \tfrac{1}{4} \qquad A_6 = \tfrac{1}{4} - K_1.$$

The remaining matrix elements can be found using the lattice symmetry:

$$B_{22}(k_x, k_y) = B_{11}(k_y, k_x) \qquad B_{23}(k_x, k_y) = B^*_{41}(k_y, k_x)$$
$$B_{24}(k_x, k_y) = B^*_{31}(k_y, k_x) \qquad B_{25}(k_x, k_y) = B^*_{61}(k_y, k_x)$$
$$B_{21}(k_x, k_y) = B^*_{51}(k_y, k_x) \qquad B_{33}(k_x, k_y) = B_{11}(k_x, k_y)$$
$$B_{34}(k_x, k_y) = B_{21}(k_x, k_y) \qquad B_{35}(k_x, k_y) = B_{51}(k_x, k_y)$$
$$B_{36}(k_x, k_y) = B_{61}(k_x, k_y) \qquad B_{44}(k_x, k_y) = B_{22}(k_x, k_y)$$
$$B_{45}(k_x, k_y) = B_{36}(k_y, k_x) \qquad B_{46}(k_x, k_y) = B_{35}(k_y, k_x)$$
$$B_{66}(k_x, k_y) = B_{55}(k_y, k_x).$$

The non-zero matrix elements S_{ij} have the form

$$S_{ii} = 1 \qquad S_{13} = A_1 = S_{24} \qquad S_{15} = \tfrac{1}{2} = S_{26} = S_{35} = S_{46}.$$

References

[1] Al Shamma F and Fuggle J C 1990 *Physica* C **169** 325
[2] Manzke R, Buslaps T, Claessen R, Skibowski V and Fink J 1990 *Phys. Scr.* **41** 579
[3] Matsuyama H, Takahashi T, Katayama-Yoshida H, Kashiwakura T, Okabe Y, Sato S, Kosugi N, Yagishita A, Tanaka K, Fujumoto H and Inokuchi H 1989 *Physica* C **160** 567
[4] Fujimori A 1990 *Physica* B **163** 736
Eisaki H, Ido T, Takagi H, Uchida S, Mizokawa T, Namatame H, Fujimori A, Tokura Y, van Elp J, Kuiper P, Sawatzky G A, Hosoya S, Katayama-Yoshida H, Oka K and Unoki H 1990 *Physica* B **165–66** 1225
[5] Picket W E 1989 *Rev. Mod. Phys.* **61** 433
[6] Wells B O, Lindberg P A P, Shen Z-X, Dessau D S, Spiecer W B and Lindau I 1989 *Phys. Rev.* B **40** 5259
[7] Romberg H, Nucker N, Alexander M, Fink J, Hahn D, Zetterer T, Otto H H and Renk K F 1990 *Phys. Rev.* B **41** 2609
[8] Varma C M, Schimitt-Rink S and Abrahams E 1987 *Solid State Commun.* **62** 681
[9] Emery V J 1987 *Phys. Rev. Lett.* **58** 2794
[10] Hirsh J E 1987 *Phys. Rev. Lett.* **59** 228

[11] Barabanov A F, Maksimov L A and Uimin G V 1988 *Zh. Eksp. Teor. Fiz. Pis. Red.* **47** 532 (Engl. Transl. 1988 *JETP Lett.* **47** 622); 1989 *Sov. Phys.–JETP* **69** (2) 371 (Engl. Transl. 1989 *Zh. Eksp. Teor. Fiz.* **96** 655)
[12] Roth L M 1988 *Phys. Rev. Lett.* **60** 379
[13] Frenkel D M, Gooding R J, Shraiman B I and Siggia E D 1990 *Phys. Rev.* B **41** 350–70
[14] Schmidt H J and Kuramoto Y 1990 *Physica* B **163** 443–56
[15] Barabanov A F, Kuzian R O, Maksimov L A and Uimin G V 1990 *Superconductivity: Phys. Chem. Technol.* **3** 8; 1989 *Progress in HTSC* vol 21, ed V L Aksenov *et al* (Singapore: World Scientific) p 477
[16] Eder R and Becker K W 1990 *Z. Phys.* B **79** 333
[17] Trugman S 1990 *Phys. Rev. Lett.* **65** 500
[18] Barabanov A F, Maksimov L A and Mikheyenkov A V 1991 *Superconductivity: Phys. Chem. Technol.* **4** 1
[19] Inui M, Doniach S and Gabay M 1988 *Phys. Rev.* B **38** 6631
[20] Emery V J and Reiter G 1988 *Phys. Rev.* B **39** 4547–56
[21] Mila F 1988 *Phys. Rev.* B **38** 11358
[22] Hybersten M S, Schluter M and Christensen N E 1989 *Phys. Rev.* B **39** 9028
[23] Arovas D P and Auerbach A 1988 *Phys. Rev.* B **38** 316
[24] Barabanov A F, Starykh O A and Maksimov L A 1990 *Int. J. Mod. Phys.* B **4** 2319–34
[25] Liang S, Doucot B and Anderson P W 1988 *Phys. Rev. Lett.* **61** 365
[26] Zhang F C and Rice T M 1988 *Phys. Rev.* B **37** 3759
[27] Takagi H, Ido T, Ishibashi S, Uota M, Uchida S and Tokura Y 1989 *Phys. Rev.* B **40** 2254
[28] Chen C-X, Schuttler M-B and Fedro A J 1990 *Phys. Rev.* B **41** 2581
[29] von Szczepanski K J, Horsh P, Stephan W and Ziegler M 1990 *Phys. Rev.* B **41** 2017
[30] Poiblanc D and Dagotto E 1990 *Phys. Rev.* B **42** 4861
[31] Moreo A, Dagotto E, Joliocoeur T and Riera J 1990 *Phys. Rev.* B **42** 6283
[32] Bacci S, Gagliano E and Nori F 1991 *Int. J. Mod. Phys.* B **5** 325
[33] Aharony A, Birgeneau R S, Coniglio A, Kastner M A and Stanley H E 1988 *Phys. Rev. Lett.* **60** 1330
[34] Jarrel M, Cox D L, Jayaprakash C and Krishnamurthy P 1989 *Phys. Rev.* B **40** 8899
[35] Ihle D and Kasner M 1990 *Phys. Rev.* B **42** 4760